

# Integration of patient-specific left atrial models for guidance in cardiac catheter ablation procedures

M.E. Rettmann<sup>1</sup>, D.R. Holmes III<sup>1</sup>, C. Dalegrave<sup>2</sup>, S.B. Johnson<sup>2</sup>, J.J. Camp<sup>1</sup>,  
B.M. Cameron<sup>1</sup>, D.L. Packer<sup>2</sup>, and R.A. Robb<sup>1</sup>

<sup>1</sup>Biomedical Imaging Resource, <sup>2</sup>Division of Cardiology/Electrophysiology, Mayo  
Clinic College of Medicine,  
Rochester, MN, USA

**Abstract.** Left atrial fibrillation is a condition in which aberrant electrical activity causes the atrium to beat rapidly and irregularly. A typical treatment strategy is to ablate a figure-eight pattern around the pulmonary veins, thereby, isolating the electrical activity of the veins from the left atrium. Thus, precise catheter guidance for targeting of these anatomical ablation sites is necessary for a successful outcome. In order to augment visualization tools such as bi-plane fluoroscopy and real-time ultrasound, recent work has focussed on incorporating detailed, patient-specific models into the procedure. In this paper, we describe work towards accurate left atrial model generation, and incorporation of these models into the cardiac ablation procedure for guidance of the catheter tip to the desired target. We present both the overall workflow as well as a case study which demonstrates our current protocol for validation of the integration procedure.

## 1 Introduction

Atrial fibrillation, a condition in which the atria of the heart beat rapidly and irregularly, is increasingly treated using minimally invasive, catheter ablation therapies. In this treatment, a catheter is guided into the left atrium and radiofrequency energy is delivered to interrupt aberrant electrical pathways. While the exact etiology of the disease is, as yet, unknown, it is believed that the ectopic foci often originate in the pulmonary veins [1]. For this reason, a typical treatment strategy is to ablate a figure eight pattern around each pair of pulmonary veins. Accurate guidance is necessary to create the appropriate lesions to eliminate fibrillation. While bi-plane fluoroscopy and real time intra-cardiac ultrasound imaging are important guidance tools, there has recently been interest in incorporating detailed, patient-specific models into the procedure [2-6]. High resolution computed-tomography (CT) or magnetic resonance (MR) scans are taken preoperatively and incorporated into the procedure by registering the real-world patient space with the image space.

We are currently developing a prototype system for cardiac ablation therapy which integrates detailed, patient-specific models, electrophysiology, and real-time catheter locations into a single user interface. In this paper, we describe the overall workflow for integrating a preoperative, patient-specific model for guidance in cardiac ablation therapy. A case study is described which demonstrates the protocol we are currently using to validate the integration procedure.

## 2 Methods

The overall workflow for integration of a patient-specific left atrial model into the ablation procedure is as follows. First, a high-resolution CT or MR scan is acquired. Next, the left atrium and pulmonary veins are segmented from the CT scan and a surface model is constructed. At the time of the procedure, the real world “patient-space” is registered with the preoperative model using a combination of landmark and surface-based registration algorithms. Once in registration, the cardiologist can use the preoperative model for navigation and target guidance.

### 2.1 System Description

Our prototype system consists of three processing/acquisition servers, a user interface, and a database [7]. In addition, our system interfaces to a commercial EP mapping system (Biosense Webster Inc., Diamond Bar, CA) which transmits locations of the tracked catheter to our system via specialized software. Each component of the system is modular and communication between the system components is through a database. This allows for a fast distributed system since the individual components can each run on separate CPUs. The user interface displays the left atrium and associated pulmonary veins segmented from the preoperative, subject specific CT data. During the procedure, the point server receives coordinate locations from the tracked catheter and the registration server registers these points to the left atrium. The user interface incorporates the most recent registration matrix to provide an updated display of the points acquired during the procedure registered to the preoperative CT data.

### 2.2 Patient-Specific Model

The preoperative model is constructed from a high-resolution CT or MR dataset. The left atrium and pulmonary veins are segmented using a validated, semi-automatic segmentation algorithm [8]. The steps of the semi-automatic method are briefly described as follows. First, seeded region growing is used to extract the blood pool using a tool in which the user can interactively adjust the threshold. This step extracts the entire blood pool including the four chambers of the heart, the pulmonary veins, aorta, superior vena cava, inferior vena cava and other surrounding structures. The next step is to separate the left atrium and

pulmonary veins from surrounding cardiac structures. This is accomplished using an algorithm that searches for thin connections between points defined by the user either in the volumetric data or on a surface rendering. This step is iteratively repeated until only the left atrium and pulmonary veins remain. A 3D tracing tool can be used to remove any extraneous pulmonary vein branches. A segmentation requires between 15 and 45 minutes of user interaction time, depending on the image quality and the level of detail desired. A snapshot of the user interface is shown in Figure 1 and an example of a segmented left atrium is shown in Figure 2.



**Fig. 1.** Interface for semi-automatic left atrial segmentation.

A validation study was conducted to assess the repeatability and accuracy of the semi-automated segmentation methodology [8]. In this study, three datasets were duplicated three times and randomized. A trained technician segmented each of the datasets using both manual tracing on image cross-sections as well as our semi-automatic technique. A second technician also segmented all nine datasets using the semi-automatic technique. The mean intra-rater repeatability of the semi-automatic technique was 5.89% and the inter-rater repeatability was 5.57%. To assess the accuracy of the semi-automatic technique, a truth model was constructed from the manually traced volumes via a pixel-by-pixel voting scheme. The mean percent difference between the semi-automated segmentation and the truth model was 3.11%. Overall, our semi-automated approach was demonstrated to be repeatable within and between raters, and accurate when compared to the truth model. The semi-automatic technique provides a substan-

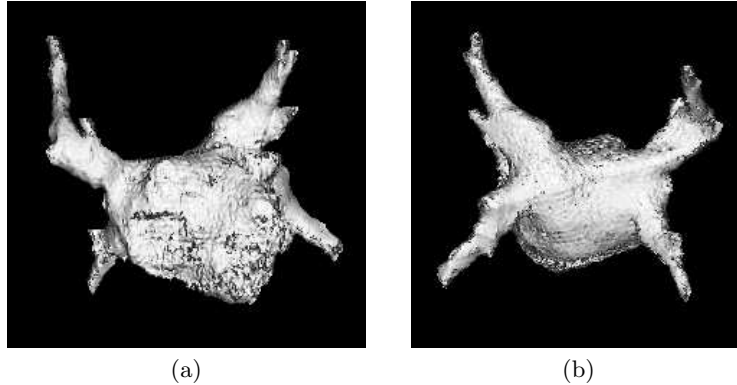


**Fig. 2.** Segmented left atrium and pulmonary veins from (a) front and (b) back view.

tial time savings (five to ten times faster) as compared with manual tracing on each image cross-section. Once the left atrium and pulmonary veins have been segmented, the binary volume is converted to a surface model using a surface tiling algorithm [9].

### 2.3 Model Integration

Accurately aligning “patient-space” with “model-space” is the key component for meaningful integration of the preoperative model into the procedure. We utilize a surface based registration approach in which points on the left atrium are sampled with the tracked catheter and used for alignment with the preoperative model. First, an initial alignment is computed using either landmark matching, or center of mass alignment. Next, a distance transform is generated from the segmented data. For each of the sampled surface points, its closest distance to the segmented structure is determined. The sum of the squared distance of all points is used as the cost metric for the downhill simplex optimization algorithm to find the best transformation matrix that minimizes this cost metric. This approach has been shown to outperform other popular surface based algorithm, such as iterative closest point (ICP) [10]. The accuracy of the algorithm was also assessed in three canine studies [11] using physical fiducial markers to obtain ground truth metrics. Absolute errors ranged from 3 to 16 mm with a mean of approximately 10 mm.

## 3 Case Study

In this section we describe an experiment which demonstrates the entire workflow for model integration as well as our current protocol for system validation in a series of animal studies. We evaluate the current registration scheme using both metrics computed during the experiment as well as additional analyses conducted retrospectively.

### 3.1 Experiment Description

A canine underwent the following procedure. First, cardiac catheters were used to place fiducial markers in the left atrium and pulmonary veins of the canine using fluoroscopic and ultrasound guidance. The fiducial markers are metal clips that are traditionally used in gastrointestinal procedures. These clips were chosen because they are visible under CT, ultrasound, and fluoroscopy, and can be delivered via a catheter. Five clips were placed throughout the left atrium and pulmonary veins. Next, a contrast-enhanced CT scan was collected with the clips in place. Figure 3 shows the locations of the clips using a maximum intensity projection rendering from the CT volume. The left atrium and pulmonary veins were segmented from the CT data and converted to a surface mesh. In addition, the location where the clip inserted into the left atrial wall was determined using the CT data. We refer to these locations as the fiducial truth points.

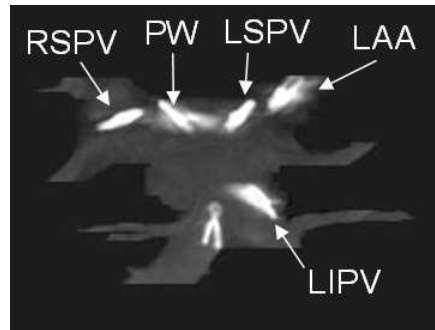


**Fig. 3.** Locations of five fiducial clips placed in the left atrium. Visualization is a maximum intensity projection viewed from the front. Clips were placed in the left atrial appendage (LAA), left superior pulmonary vein (LSPV), left inferior pulmonary vein (LIPV), right superior pulmonary vein (RSPV), and one along the posterior wall (PW) of the left atrium. One clip did not attach to the atrial wall and can be seen floating near the right inferior pulmonary vein.

A follow-up procedure was conducted to evaluate registration accuracy and the ability to guide using the preoperative surface model only. First, the alignment between patient-space and image space was computed. The registration was initialized using a landmark matching algorithm with 7 landmark pairs. Anatomical landmarks were located in the left atrium under bi-plane fluoroscopy and ultrasound guidance. The locations of these points were recorded by our system via the tracked catheter output from the commercial Biosense system. The corresponding locations were identified on the surface model. Next, approximately 30 surface points were collected which were used to iteratively refine the registration. The computed transformation matrix is used to align both the

tracked catheter and any points sampled by the catheter to the preoperative left atrial model.

Once in registration, the monitor for our system was turned off and the cardiologist navigated to each fiducial using bi-plane fluoroscopy and ultrasound for guidance. When the catheter was on the clip, the location was recorded with our system. The location of this point is then transformed by the current registration matrix to put it into the model space. We refer to this location as the fiducial sampled points. This process was repeated three times in order to assess repeatability of catheter placement. Figure 4 shows a snapshot of the interface after the catheter tip was navigated to a fiducial clip under fluoroscopic and ultrasound guidance. This visualization was not available to the cardiologist, but was monitored by our technical team in order to qualitatively assess the accuracy and usability of our system interface.

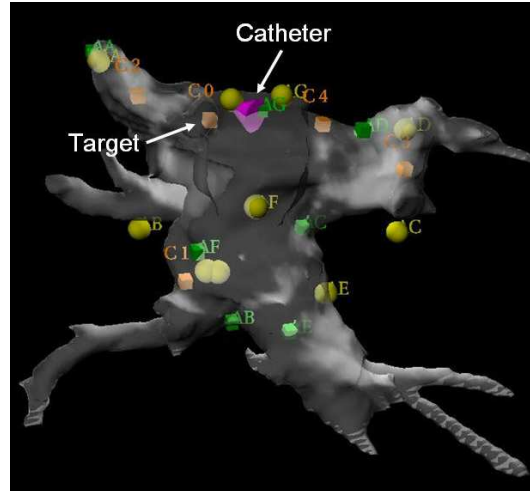


**Fig. 4.** A snapshot of the interface after the catheter tip was navigated to a fiducial clip under fluoroscopic and ultrasound guidance. The surface model is shown semi-transparent in white, the surface points as yellow balls, the fiducial clips as orange cubes, and the catheter as a magenta cone.

In the second phase of the experiment, the cardiologist used only our system interface for visual navigation, that is, ultrasound and fluoroscopy were shut off. For each fiducial clip, the cardiologist navigated to the target which was represented as an orange cube in our interface. Once on the target, a radiofrequency burn was made in the left atrial tissue. Following the procedure, the left atrium was dissected and the distance between the insertion point of the clip and the tissue lesion was measured. Measurements were made to both the center and edge of the burn. Measured errors were as follows: 0.0/2.0 mm (LAA), 4.5/8.8

mm (LSPV), 0.0/2.0 mm (LIPV), 2.6/5.5 mm (RSPV), 0.0/4.4 mm (posterior wall) where the first value indicates distance to edge and the second value indicates distance to center. A distance of 0.0 indicates that the clip insertion point was encompassed by the burn lesion.

### 3.2 Retrospective Analyses

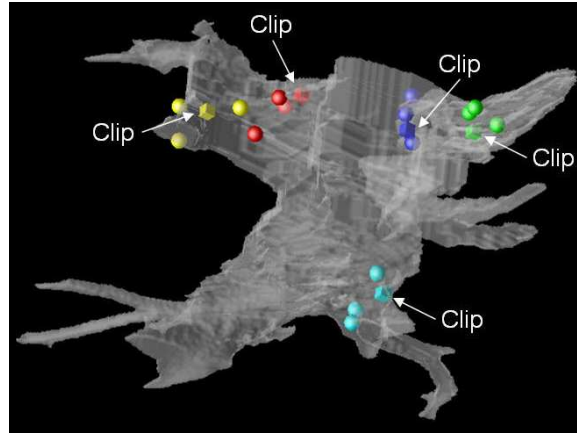
Several retrospective analyses were conducted on the data collected during the experiment. First, the quantitative registration errors were computed for the first part of the experiment where the registration error is computed as the difference between the fiducial sampled point and the fiducial truth points. For each fiducial truth point, three sampled points were independently collected by the cardiologist by guiding the catheter to the clip under fluoroscopy and ultrasound guidance. The transformed, sampled fiducial points are shown along with the fiducial truth points in Figure 5. The sampled fiducial points are shown as spheres and the true clip locations are shown as cubes. Overall, the sampled locations align well with the true clip locations. Mean errors for each clip were as follows: 7.7 mm (LAA), 4.8 mm (LSPV), 5.8 mm (LIPV), 6.1 mm (RSPV), 6.9 mm (posterior wall).

In order to obtain an estimate of the lower bound achievable for the fiducial errors, we computed the least squares fit between the fiducial truth points and the fiducial sampled points. The mean residual errors for the three visits to each clip are as follows: 3.4 mm (LAA), 3.5 mm (LSPV), 3.2 mm (LIPV), 2.9 (RSPV) mm, 3.4 mm (posterior wall). In theory, these error should be zero, but there are several sources of potential errors for a perfect alignment including accurate placement of the catheter tip on the clip insertion point under fluoroscopy and ultrasound guidance, respiratory motion between the acquired CT scan and the point sampled during the procedure, and accurate location of the clip insertion point in the CT data. The challenge of locating the clip insertion point is demonstrated in Figure 6. The clips create star shaped image artifacts in the CT data as shown in Figure 6(a). In order to determine the insertion point, the clip was followed through slices in the CT data until it appeared to insert into the tissue as indicated by the arrows in Figure 6(c).

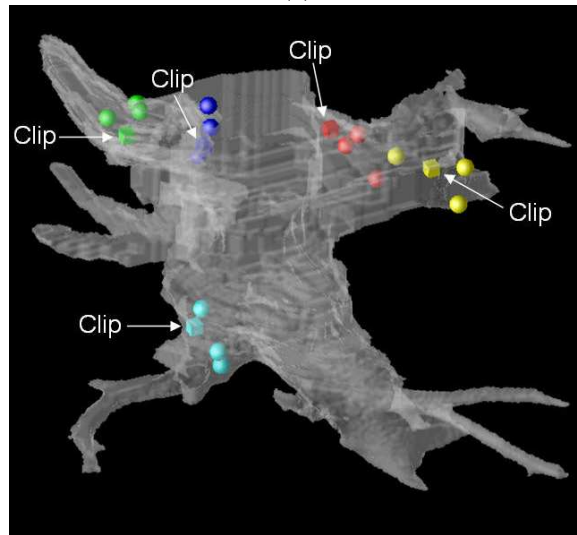
## 4 Discussion

In this paper, we have described the complete workflow required to incorporate a patient-specific preoperative model into an image-guided cardiac ablation procedure. The key steps include accurate segmentation of left atrial and pulmonary vein anatomy for model construction, registration of real-world patient space with model space, and visualization tools that are usable and intuitive. In previous work, we have validated our segmentation and registration algorithms, however, this is the first report of using our prototype system for guidance.

We have described an end-to-end protocol for validation of guidance and targeting using our prototype system. We are currently using this protocol in



(a)



(b)

**Fig. 5.** Registration of fiducial sampled points to fiducial truth points from (a) front and (b) back views of the left atrium. The left atrial surface model is shown semi-transparent in white. Truth points, which are the physical fiducial clips, are represented as cubes and the registered, sampled points are represented as spheres. The cardiologist navigated to each clip three times, each independent navigation is a separate sphere. Color scheme is as follows: green=LAA, blue=LSPV, cyan=LIPV, yellow=RSPV, red=posterior wall.

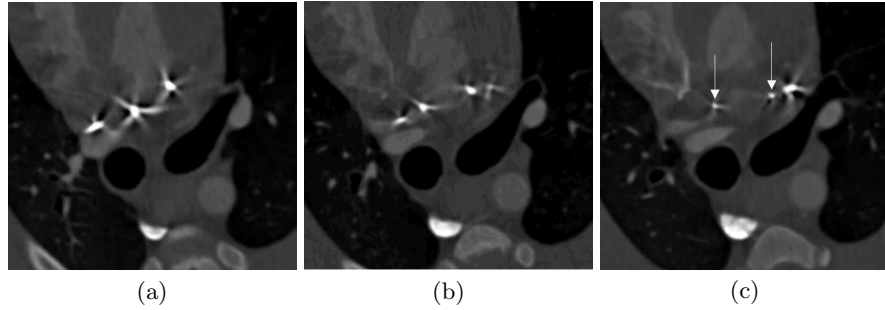


**Fig. 6.** Locating clip insertion points in CT data. Clips were followed through image slices (a)-(b) until they appeared to insert into the tissue as indicated by the arrows in (c).

a series of canine experiments with the intent to quantify both the total guidance accuracy of our system, as well as to tease apart the various error sources that comprise this final error. In the first half of the experiment, the cardiologist navigated to each fiducial clip under standard guidance tools (fluoroscopy and ultrasound) and we monitored the visualizations from our system for usability and accuracy. Post-procedure, we computed the quantitative error metrics. Several error sources could potentially contribute to these fiducial errors including: accurate placement of the catheter on fiducial clip using fluoroscopy and ultrasound guidance, cardiac motion, respiratory motion, and accuracy of the registration algorithm.

While accuracy of catheter tip placement cannot be directly assessed, reproducibility can be studied by repeat visits to the fiducial locations. In our experiments, cardiac motion is at least partially compensated by acquiring the CT scan at approximately the same point in the cardiac cycle that the commercial system collects points. Currently, however, there is no compensation for respiratory motion. In future work, we hope to track respiration and map all points back to end expiration, which corresponds to the respiratory phase of the CT scan.

In the second half of the experiment, the cardiologist navigated to each fiducial clip using only our system for guidance. Potential sources of error in this phase of the experiment include: the ability to accurately locate the target insertion point in the CT data, ability to visualize and navigate using our system interface, respiratory motion, cardiac motion, and error in the registration algorithm. Navigation to a designated target location can prove challenging in three-dimensional data since the model must be visualized from various angles to insure that the catheter tip is indeed directly on the target. In future experiments, we intend to evaluate various visualization strategies to determine if one provides better targeting capabilities over others.

Our overall goal in this project is to provide a prototype system for image-guided cardiac ablation therapy that improves visualization tools available to the

cardiologist. We believe that incorporation of detailed patient-specific models could improve the procedure, provided the integration is done in an accurate, useful, and intuitive fashion. Improvements would include reduced procedure time, reduced fluoroscopy exposure to the patient and cardiologist, and finally, more accurate targeting of the ablation sites.

### Acknowledgements

This research was supported by NIH grant RO1EB002834 from the National Institute of Biomedical Imaging and Bioengineering.

### References

1. Blaauw, Y., Crijns, H.: Atrial fibrillation: insights from clinical trials and novel treatment options. *Journal of Internal Medicine* **262** (2007) 593–614
2. Dickfeld, T., Calkins, H., Zviman, M., Kato, R., Meininger, G., Lickfett, L., Berger, R., Halperin, H., Solomon, S.: Anatomic stereotactic catheter ablation on three-dimensional Magnetic resonance images in real time. *Circulation* **108** (2003) 2407–2413
3. Lacomis, J., Wigginton, W., Fuhrman, C., Schwartzman, D., Armfield, D.R., Pealer, K.: Multi-detector row CT of the left atrium and pulmonary veins before radio-frequency catheter ablation for atrial fibrillation. *RadioGraphics* **23** (2003) S35–S50
4. Mansour, M., Holmvang, G., Ruskin, J.: Role of imaging techniques in preparation for catheter ablation of atrial fibrillation. *J. Cardiovasc Electrophysiol* **15** (2004) 1107–1108
5. Reddy, V., Malchano, Z., Holmvang, G., Schmidt, E., d’Avila, A., Houghtaling, C., Chan, R., Ruskin, J.: Integration of cardiac magnetic resonance imaging with three-dimensional electroanatomic mapping to guide left ventricular catheter manipulation. *Journal of the American College of Cardiology* **44**(11) (2004) 2202–13
6. Sun, Y., Azar, F., Xu, C., Hayam, G., Preiss, A., Rahn, N., Sauer, F.: Registration of high-resolution 3D atrial images with electroanatomical cardiac mapping: Evaluation of registration methodology. In: *SPIE Medical Imaging*. (2005) 299–307
7. Rettmann, M., III, D.H., Su, Y., Cameron, B., Camp, J., Packer, D., Robb, R.: An integrated system for real-time image guided cardiac catheter ablation. In: *Stud Health Technol Inform.* (2006) 455–60
8. Rettmann, M., III, D.H., Camp, J., Packer, D., Robb, R.: Validation of semi-automatic segmentation of the left atrium. In: *Proceedings of SPIE – Volume 6916*. (2008)
9. Lin, W., Robb, R.: Dynamic volume texture mapping and model deformation for visually realistic surgical simulation. In: *Proceedings of Medicine Meets Virtual Reality*. Volume 62. (1999) 198–204
10. Su, Y., III, D.H., Rettmann, M., Robb, R.: A piecewise function-to-structural registration algorithm for image guided cardiac catheter ablation. In: *SPIE Medical Imaging*. (2006)
11. Rettmann, M., III, D.H., Su, Y., Kolasa, M., Johnson, S., Packer, D., Robb, R.: Evaluation of global versus piecewise registration using a ground truth canine model. In: *IEEE International Symposium on Biomedical Imaging: From Nano to Macro*. (2006)